

In-Situ Measurement of Fracture Toughness for Safe Conversion of Existing Pipelines to Hydrogen Service

Xuejun Huang¹, Intisar Rizwan i Haque¹, Victor Jablovkov¹, Simon Bellemare¹

¹Massachusetts Materials Technologies, LLC



**19TH PIPELINE
TECHNOLOGY
CONFERENCE**
8-11 APRIL 2024, BERLIN

Organized by



Proceedings of the 2024 Pipeline Technology Conference (ISSN 2510-6716).

www.pipeline-conference.com/conferences

Copyright ©2024 by EITEP Institute.

1 ABSTRACT

Hydrogen blending into natural gas pipelines has been proposed as a possible solution for delivering low-carbon energy to the urban market while leveraging the existing infrastructure. One of the concerns is that hydrogen may lower the fracture toughness of pipeline steels. Recent research has demonstrated that risk but also provided insight into how variable service conditions and variable characteristics of vintage steel can lead to a range of low to high risks depending on the assets. Measuring the fracture toughness of hydrogen embrittled steels can be complicated and usually requires destructive cutouts and laboratory tests. This paper presents a potential solution where pipe toughness is measured in-situ through a surface test using a new method, planing-induced microfracture. It involves using a specialized blade, featuring a central opening, to plane the surface of a material. As the blade moves across the surface, the material at the central opening is not machined but rather deformed in tension until fracture. Characteristics of residual ligaments on the cut surface of the substrate and the opposite face of the separated chip are correlated with the material's fracture toughness. Results from a proof-of-concept lab test that implements this method and the development of a field prototype will be presented in this paper. This method will facilitate pipeline integrity assessment and support the introduction of hydrogen blends into existing pipelines.

2 INTRODUCTION

Hydrogen emerges as a pivotal element in the pursuit of decarbonization, offering a sustainable alternative to traditional fossil fuels. Its integration into the energy matrix is crucial for achieving global carbon neutrality goals. However, hydrogen transportation poses significant challenges, necessitating innovative and practical solutions. Leveraging existing natural gas pipeline infrastructure presents a promising near-term approach to address this logistical hurdle [1]. Yet, this solution is not without its complexities. A primary concern in this endeavor is hydrogen embrittlement, a phenomenon adversely affecting the integrity of pipeline steel. This embrittlement can compromise pipelines' structural and functional reliability, raising critical safety and operational concerns.

The hydrogen embrittlement effect on pipeline steels in a gaseous hydrogen environment has been studied extensively in recent years. In general, the fracture toughness of pipeline steels in hydrogen gas decreases with an increase in hydrogen partial pressure or fugacity. There appears to be no lower threshold for hydrogen partial pressure required for hydrogen embrittlement [2]. In other words, for a transmission pipeline, any partial pressure or percentage of hydrogen in the blend would reduce the materials' fracture toughness. For example, Ronevich and San Marchi [3] observed an approximately 6.7% reduction in fracture toughness of X52 pipeline steel in 3% hydrogen with a total pressure of 3.4 MPa (the rest being nitrogen), and this number increases to 50% when the total pressure increases to 21 MPa with the same hydrogen percentage. A similar effect of hydrogen has been observed by Nguyen et al. [4] on X70 pipeline steel.

Notably, a reduction in fracture toughness does not necessarily render the pipeline unfit for service. The failure pressure can be estimated using the failure assessment diagram (FAD) following API 579-1/ASME FFS-1. Using specific models, it is shown that in the absence of significant defects, the failure pressure of modern pipeline steels could remain relatively unchanged even if the fracture toughness is halved [5]. This is consistent with the "optimal toughness" concept described in API 1176. If the reduced fracture toughness is still beyond the optimal toughness, degradation in failure pressure would be minimal.

However, most existing pipelines are built in earlier years and are likely to have lower fracture toughness in which case the failure pressure would be affected by hydrogen blending [5]. Literature has shown that the fracture resistance of pipe steels tends to exhibit a negative power law relationship

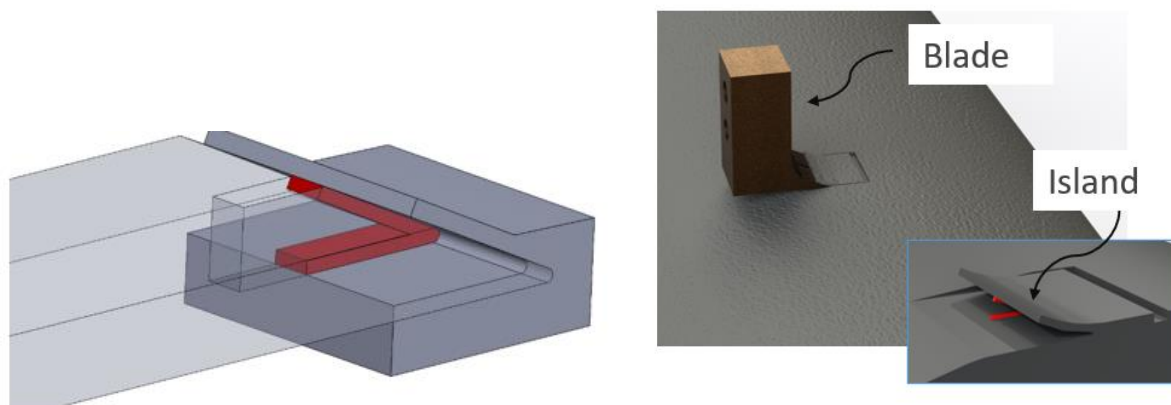
with hydrogen fugacity. However, the slope of this trend varies across different steel grades [6]. If such a trend can be tabulated for each grade of steel, it would enable operators and engineers to predict the diminished fracture toughness of steel when subjected to varying hydrogen blending ratios, provided the initial fracture toughness is known. Unfortunately, fracture toughness was not assessed at construction time for most vintage pipelines. Current methods to measure the fracture toughness of pipeline steels use destructive testing such as Charpy V-Notch impact energy or fracture mechanics testing. Obtaining samples for these tests requires cutouts, an expensive process that may require service interruption and can lead to gas release.

This paper introduces an innovative, in-situ, and minimally invasive testing method called planing-induced microfracture to collect pipe toughness data. This method aims to facilitate the evaluation of the structural integrity of existing pipelines, including in the context of hydrogen blending.

2.1 PLANING-INDUCED MICROFRACTURE METHOD

Developed in 2022, planing-induced microfracture introduces a sub-surface microcrack into the material and measures its features, correlating to the material fracture toughness. It uses a specialized blade featuring a central opening to plane the surface of a material (Figure 1). As the blade moves across the surface, the material at the central opening is uncut. Material in this region flows through the opening and is subjected to tensile stress until it fractures. This opening is referred to as the "stretch passage," as the material passing through it experiences primarily tensile strain. When the material fractures, residual ligaments remain on the cut surface of the substrate and the opposite face of the separated chip. The characteristics of these ligaments, such as their height and the crack front within the stretch passage, correlate with the material's fracture toughness, as discussed later in this paper.

Figure 1. Left: Planing-induced Microfracture Concept. Right: Schematic of Field Implementation



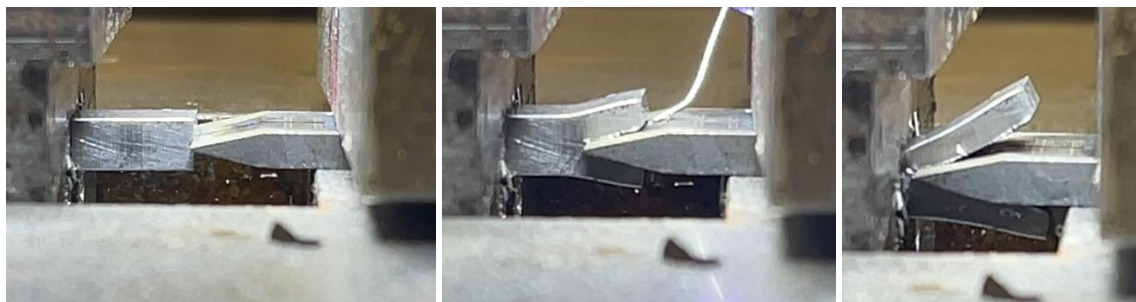
3 PROOF-OF-CONCEPT VALIDATION TESTING

To test the planing-induced microfracture idea and establish a correlation to fracture toughness, an initial proof-of-concept validation test was performed on a simplified test apparatus that utilized the same blade concept and "cut" the sample in halves instead of "planing". The process is detailed in a previous paper [7] and will be briefly mentioned here. Additional processing and modeling development since then will be discussed.

3.1 PROOF-OF-CONCEPT TEST SETUP

The laboratory setup consists of a tungsten carbide blade configured to drive into the center of a machined sample of pipeline steel at a constant speed of 5 mm per minute (Figure 2). The tungsten carbide blade has a 25-degree angle split evenly about the cutting edge, and a “stretch-passage” of 0.76 mm in width. The pipeline steel samples utilized in this study were machined from 30 different pipe cutouts, with a dimension of 3.18 mm thickness, 6.35 mm width, and 7.62 mm length. For each pipe cutout, 2-4 specimens were machined and tested.

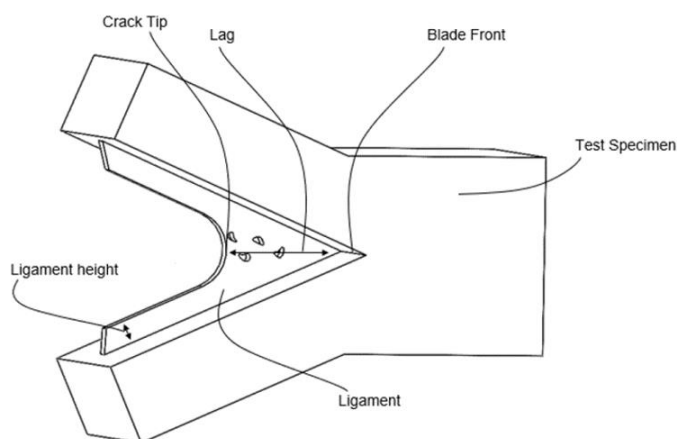
Figure 2. Proof-of-Concept Test (Left: Test Start Point. Middle: Test Midpoint. Right: Test End Point.)



3.2 MEASUREMENT OF CRACK FEATURES

Once the microcrack has been successfully generated, efforts have been made to measure features of the crack and establish a correlation to the material fracture toughness. So far, two features have exhibited a good correlation to fracture toughness: the total ligament height and the lag measurement (Figure 3). The total ligament height is the sum of the ligament height on each side of the fractured specimen, measured from the cut plane. The lag measurement is the distance between the crack tip and the blade edge at the test midpoint. The details of lag measurement are given in Section 3.2.2.

Figure 3. Schematic of the Cracked Specimen

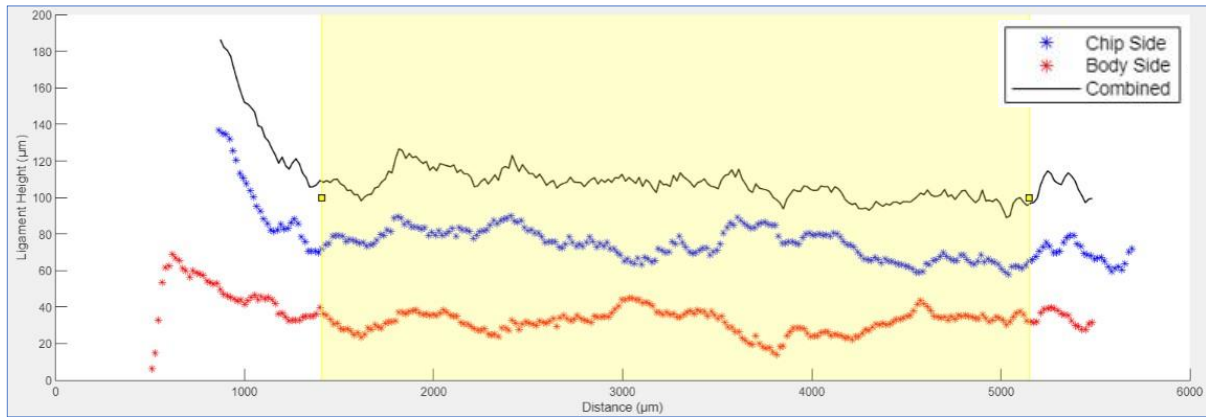


3.2.1 Ligament Height Measurement

Ligament height on each side of the fracture specimen is measured using a laser scanning system described in [7]. The two ligament height profiles are aligned using internally developed software. This alignment process eliminates many variations on each side and achieves a smoother total ligament height profile. The initial region is typically an increased height corresponding to the initial tensile

response leading up to the generation of the fracture. After this fracture begins to propagate, the height of the ligament stabilizes and reaches a region highlighted in yellow referred to as the 'steady-state region' (Figure 4). Finally, as the test reaches the back of the sample, the behavior becomes more erratic as edge effects come into play. The average ligament height in the steady-state region is calculated and used in the later analysis.

Figure 4. Ligament Height Processing



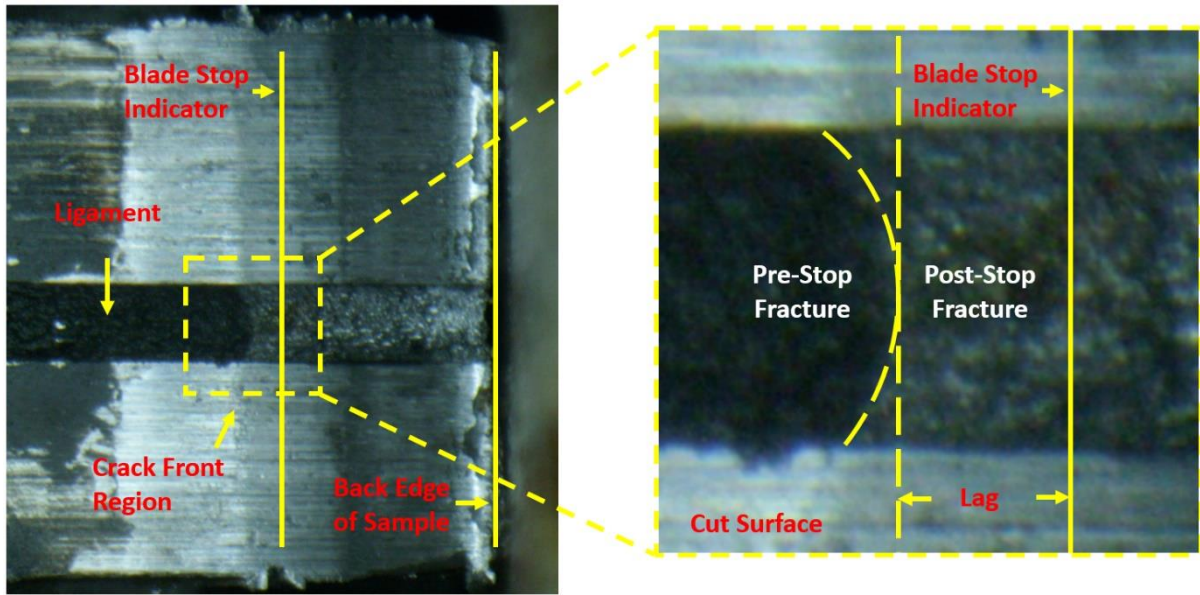
3.2.2 Lag Measurement

The relative position of the crack front to the position of the blade edge is another critical output of the planing-induced microfracture test. To measure this feature, images are taken using an AmScope H1000 Microscope mounted in a fixed position above the test. An image is taken at the mid-point of the test (Figure 2 (b)), where the blade movement is stopped and when the black oxide coating is allowed to develop in the stretch passage. During post-processing, the distance from the forward-most point of the blade to the back edge of the sample in this image is recorded for use. Once the test is completed and the sample is separated into two pieces, each revealed sample surface is imaged utilizing the same setup.

Figure 5 (a) shows an example of the processed image. The processing software user positions the yellow line to match the location of the blade when the blade movement is stopped and when the black oxide layer is developed. This line can be placed accurately by measuring from the sample's back edge in the image taken during the black oxide layer development. The yellow highlighted rectangular box close to the center of the image is used to refine the portion of the image passed onto the next processing stage.

Once the image is refined to just the crack front region, the actual crack front is identified and segmented into five equal parts. The lag measurement is the difference between the average crack front position in the center region and the blade edge position. Note that the value can be positive (crack front lags blade edge) or negative (crack front exceeds blade edge).

Figure 5. Left: Processed Post Test Image. Right: Schematic of Lag Measurement



4 FRACTURE TOUGHNESS MODELS AND RESULTS

A physical model correlating ligament height to fracture toughness has been established [7]. This model assumes that the ligament height (LH) is linearly related to the elongation at break (ϵ_f), i.e.,

$$\epsilon_f = a * LH + b$$

From Oh [8], the fracture toughness (K_{Ic}) is related to the toughness measured using the area under the tensile stress-strain curve up to the elongation at break (K_f):

$$(K_{Ic}/\sigma_y)^2 = \alpha (K_f/\sigma_y)^2$$

And K_f can be evaluated using the yield strength, ultimate tensile strength (σ_u), and elongation at break (ϵ_f):

$$K_f \approx \epsilon_f [k\sigma_y + (1 - k)\sigma_u]$$

Where k is a weighted coefficient to account for the nonlinearity of the stress-strain curve and $0 < k < 1$. Using these relations, ligament height can be correlated to K_{Ic} in the following form [7]:

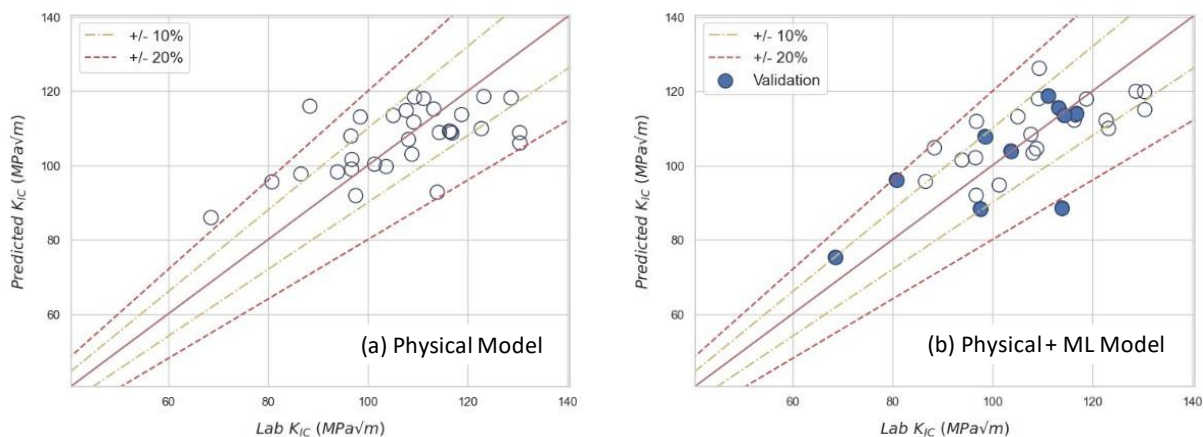
$$K_{Ic}/\sigma_y = C_1 * [k + (1 - k)\sigma_u/\sigma_y] * LH + C_2/\sigma_y + C_3$$

where C_1 , C_2 , C_3 , and k are fitted coefficients using test data. A unity plot (predicted K_{Ic} vs. destructive lab-tested K_{Ic}) resulting from this physical model using the validation test data is shown in Figure 6 (a).

A machine learning (ML) model is built in addition to the physical model to improve the prediction accuracy. The output of the physical model (predicted K_{Ic}), the lag measurement, the selected chemical composition of the material and grain size are used as inputs to the machine learning model. The result from the machine learning model is shown in Figure 6 (b). Significant improvement can be observed from the physical + ML model. For all but one data point the predicted K_{Ic} values are within $\pm 20\%$ of the lab-tested values, and approximately 75% of the data points are within $\pm 10\%$.

The unity plot in Figure 6 shows 30 samples. 21 samples were used to train the machine learning model, and the remaining ten samples were used to validate the ML model shown in blue circles in Figure 6 (b). Only four features were used as ML Model inputs to ensure that the ML model was not overfitting to the available data. The use of ML models on top of the physical model decreases the error by 14% when all 30 samples are considered.

Figure 6. (a) Physical Model Result. (b) Physical+ML Model Result.



5 FIRST GENERATION FIELD INSTRUMENT

MMT is currently building a field instrument called the Blade Toughness Meter (BTM) that utilizes the planing-induced microfracture method [7]. The BTM instrument (Figure 7) is a standalone device that allows the operator to attach to a live pipeline from 0.20 to 1.22 meters in diameter.

To perform a BTM test on a pipe, the pipe surface must be prepared with samples that the blades can plane off. These samples are referred to as “islands”. The islands are generated using a milling assembly that can translate forward and backward along the main ‘T’ of the frame (Figure 7). The milling tool position is locked at six prescribed locations where a custom-made non-plunging bit is utilized to machine the island feature at each location where the milling depth is controlled with a noncutting surface at bottom surface of the tool (Figure 8). The spacing of the six drilling locations is such that the overlap results in four slightly curved rectangular islands (Figure 9).

After all four islands are machined each side of the island is then tested with two independent test apparatuses, allowing a total of eight tests. Each test apparatus consists of a movable drive mechanism that holds the test blade and is driven at a precise and constant speed via a stepper motor (Figure 10). Upon completion of the 8 tests, the mag drill is reinstalled with a “clean up end mill” which removes any sharp edges remaining from the initial surface machine and subsequent testing that could result in stress concentrations from the pipe’s internal pressure.

Figure 7. Field Prototype of Blade Toughness Meter (BTM)

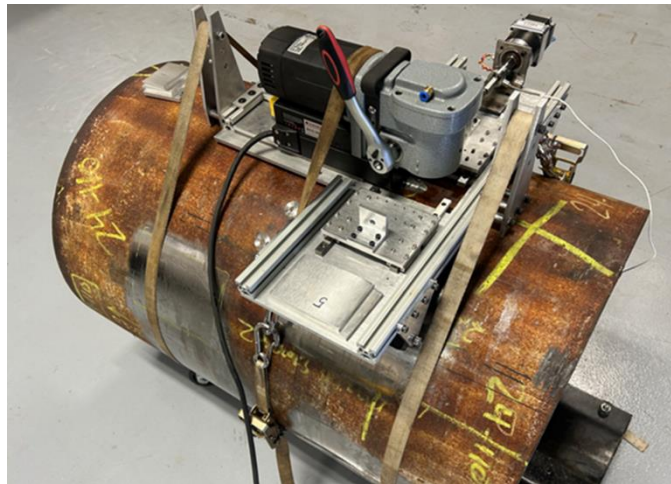


Figure 8. Schematic of the Milling Assembly that Generates “Islands” on a Pipe Surface (Top View)

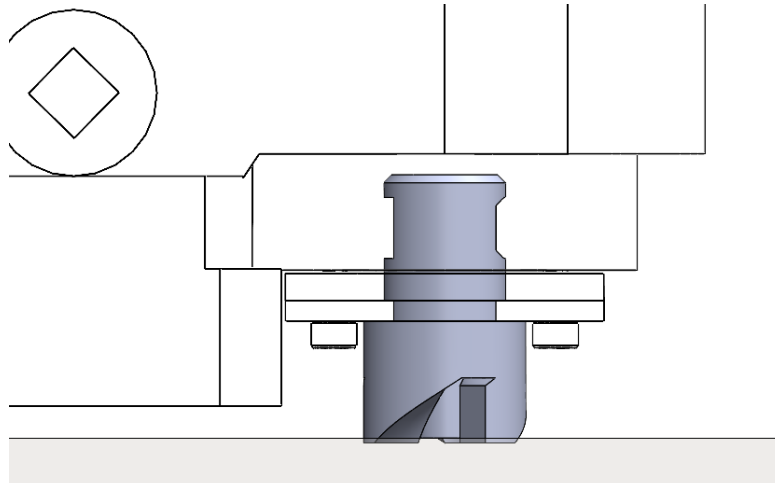


Figure 9. Example of Prepared Islands



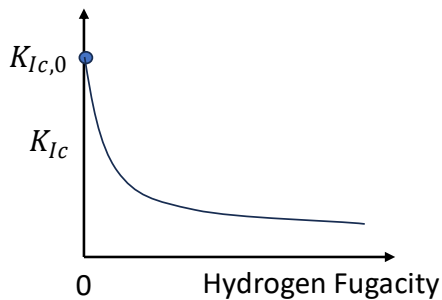
Figure 10. BTM Testing with the Field Instrument



6 APPLICATION TO HYDROGEN BLENDING EVALUATION

Studies [2][3][6] have shown that fracture toughness reduces significantly with hydrogen fugacity following a negative power law dependence (Figure 11). The shape of this curve varies with different types of steel including pipe grades and other manufacturing characteristics [6].

Figure 11. Left: Schematic of K_{Ic} vs. Hydrogen Fugacity Curve. Right: Pseudo Tabulated Reduced Factors for a grade of steel.



Hydrogen Fugacity (MPa)	Reduction Factor
1	0.95
5	0.85
10	0.70
30	0.64
50	0.60

When this trend is tabulated as reduction factors (RF) at different hydrogen fugacity levels (f_H) for a steel grade, the fracture toughness of a pipe exposed to hydrogen can be estimated as

$$K_{Ic} = K_{Ic,0} * RF(f_H)$$

When evaluating the feasibility of blending hydrogen into existing gas pipelines, the following procedure is proposed:

- Measure $K_{Ic,0}$ using the proposed planing-induced microfracture method at the required spatial frequency throughout the piping network.

- Identify a desired hydrogen blending ratio, calculate the hydrogen fugacity [5] and find the corresponding reduction factor applicable to the type of pipeline steel.
- Calculate K_{Ic} applicable to the inside of the pipeline using the data from the $K_{Ic,0}$ data from testing the outside and the applicable reduction factor.
- Estimate the maximum flaw size that could exist in the piping network.
- Determine the failure pressure using the failure assessment diagram (FAD) [5]. Note that with hydrogen blending, the slope of the loading path becomes $1/RF$ of the original slope when material yield strength remains relatively unchanged with hydrogen [9]. In general, this results in a lower failure pressure unless the intersection of the loading path is on the vertical section of the FAD curve.

This procedure can be repeated with different targeted hydrogen blending ratios and determine the most desirable hydrogen level.

7 CONCLUSIONS

A proof-of-concept lab test implementing the planing-induced microfracture method was validated with 30 pipe samples. Physical and machine learning models were built to correlate the microcrack features to the material fracture toughness K_{Ic} . Preliminary results show that almost all predicted K_{Ic} values fall within $\pm 20\%$ of the lab-tested values, and the majority are within $\pm 10\%$.

A first generation of the field instrument has been designed and successfully performed tests on a pipe cutout. Future work includes full validation of the field instrument to perform pipeline material verification before utilization on live pipes.

The proposed method provides an in-situ, fast, and minimally invasive way to measure the fracture toughness of pipeline steels. When combined with an appropriate reduction factor depending on the targeted blending ratio, it enables the calculation of the failure pressure and further techno-economic analysis. This method will help operators in their considerations of hydrogen blending and offer tremendous cost-saving opportunities compared to conventional lab testing.

8 REFERENCES

[1] Topolski, Kevin, et al. "Hydrogen blending into natural gas pipeline infrastructure: review of the State of technology." (2022).

[2] Briottet, Laurent, and Hamza Ez-Zaki. "Influence of hydrogen and oxygen impurity content in a natural gas/hydrogen blend on the toughness of an API X70 steel." Pressure Vessels and Piping Conference. Vol. 51685. American Society of Mechanical Engineers, 2018.

[3] Ronevich, Joseph A., and Chris San Marchi. "Materials compatibility concerns for hydrogen blended into natural gas." Pressure Vessels and Piping Conference. Vol. 85345. American Society of Mechanical Engineers, 2021.

[4] Nguyen, Thanh Tuan, et al. "Fracture properties and fatigue life assessment of API X70 pipeline steel under the effect of an environment containing hydrogen." Journal of Mechanical Science and Technology 35.4 (2021): 1445-1455.

[5] Kappes, Mariano A., and Teresa Perez. "Hydrogen blending in existing natural gas transmission pipelines: a review of hydrogen embrittlement, governing codes, and life prediction methods." Corrosion Reviews 0 (2023).

[6] San Marchi, Chris, et al. "Fracture resistance and fatigue crack growth of X80 pipeline steel in gaseous hydrogen." Pressure Vessels and Piping Conference. Vol. 44564. 2011.

[7] Huang, Xuejun, et al. "Validation of Planing-Induced Microfracture for Determining Pipe Body Toughness." Pressure Vessels and Piping Conference. American Society of Mechanical Engineers, 2024. Submitted.

[8] Oh, Gyoko. "A simplified toughness estimation method based on standard tensile data." International Journal of Pressure Vessels and Piping 199 (2022): 104733.

[9] San Marchi, Christopher W., and Brian P. Somerday. Technical reference for hydrogen compatibility of materials. No. SAND2012-7321. Sandia National Laboratories (SNL), Albuquerque, NM, and Livermore, CA (United States), 2012.